

Cite this article as: Tian Zhenyun, Chen Liangbin, Song Jingjing, et al. Preparation of Ti-Al Alloys by Aluminothermic Reduction with MgF_2 Addition[J]. Rare Metal Materials and Engineering, 2025, 54(07): 1678-1686. DOI: <https://doi.org/10.12442/j.issn.1002-185X.20240346>.

ARTICLE

Preparation of Ti-Al Alloys by Aluminothermic Reduction with MgF_2 Addition

Tian Zhenyun¹, Chen Liangbin¹, Song Jingjing², Kang Jialong¹, Mao Hongxia¹, Qiu Guibao^{1,3}

¹College of Materials Science and Engineering, Chongqing University, Chongqing 400044, China; ²Chongqing Academy of Metrology and Quality Inspection, Chongqing, 401121, China; ³Chongqing Key Laboratory of Vanadium – Titanium Metallurgy and New Materials, Chongqing University, Chongqing 400044, China

Abstract: The Ti-Al alloy was synthesized using the aluminothermic reduction of TiO_2 , with CaO and MgF_2 serving as flux components. Investigations were conducted to ascertain the effects of MgF_2 content on the alloy-slag separation, alloy microstructure, composition, phase constitution, overall alloy yield, and aluminothermic reduction of TiO_2 . Results indicate that MgF_2 enhances the separation of the alloy from slag and promotes the formation of the TiAl phase within the alloy matrix. Nevertheless, an overabundance of MgF_2 reduces the interfacial tension between the Al reductant and the slag, leading to significant loss of Al. This adversely affects alloy-slag separation, escalates the incorporation of oxide inclusions in the alloy, and severely reduces the recovery rate of alloy. Concurrently, the alloy has a phase transition from TiAl to Ti_3Al . The optimum condition for alloy-slag separation and alloy integrity is realized at the MgF_2 content of 10wt%. Kinetic analysis at this flux ratio determines the activating energy for the Al- TiO_2 -CaO- MgF_2 system, which is 409.729 kJ/mol, and the order of kinetics is $n=0.38$.

Key words: MgF_2 ; Ti-Al alloy; alloy-slag separation; aluminothermic reduction

1 Introduction

Titanium is a metal renowned for its excellent attributes of low density, high strength, and outstanding corrosion resistance^[1-2]. However, the effectiveness of pure titanium is restricted under extreme conditions. Through the creation of titanium alloy achieved by the incorporation of other metal elements, its performance and application could be improved. Aluminum is often used as an α -phase stabilizer in titanium metal, reinforcing its mechanical strength and holding reliable performance in high-temperature settings^[3]. Alloys synthesized by titanium and aluminum maintain significant strength and exhibit superior oxidation resistance at high temperature, making them particularly suitable for high-temperature aerospace engine components that require stringent maintenance of both structural integrity and thermal resistance^[4-5]. The high-temperature capabilities of Ti-Al alloys are comparable to those of sophisticated high-

temperature steels and nickel-based superalloys. Moreover, Ti-Al alloys possess a significant advantage, their density is roughly half that of nickel-based superalloys^[6]. The lower density reduces engine mass, indirectly enhancing auxiliary component longevity, lowering costs, and cutting energy use. Consequently, Ti-Al alloys are considered the next-generation material for future aviation advancements^[7-8].

Currently, the manufacture of Ti-Al alloys encompasses several methods, including casting, ingot metallurgy (IM), and powder metallurgy (PM)^[9-10]. The microstructure of Ti-Al alloy fabricated by casting is typically coarse, and the process is prone to solidification defects, such as shrinkage porosity and cavities. The advent of hot isostatic pressing (HIP) technique has significantly improved the quality of alloys produced via casting^[11]. IM process prepares Ti-Al alloy ingots by melting titanium and aluminum, subsequent to which the ingots endure HIP and homogenization annealing

Received date: June 06, 2024

Foundation item: National Natural Science Foundation of China (52074052)

Corresponding author: Qiu Guibao, Ph. D., Professor, College of Materials Science and Engineering, Chongqing University, Chongqing 400044, P. R. China, E-mail: qiuguibao@cqu.edu.cn

Copyright © 2025, Northwest Institute for Nonferrous Metal Research. Published by Science Press. All rights reserved.

treatments^[12]. However, Ti-Al alloy ingots produced through conventional melting processes frequently exhibit problems with microstructural uniformity and compositional segregation^[13-14]. Typically, a more consistent microstructure is achievable through repeated vacuum arc remelting of the ingot at the expense of increased energy consumption. Compared to the above two methods, PM process offers a pathway for Ti-Al alloy by powder raw material. This technique bifurcates into the elemental powder metallurgy (EPM) and the pre-alloyed (PA) methods^[15]. EPM entails blending titanium and alloy element powders, and vacuum sintering to form the alloy^[16]. PA process involves melting alloying elements with sponge titanium, preparing pre-alloying powder through atomization, and then using HIP technique to prepare titanium alloy, which is more complex than EPM process^[17]. Nevertheless, this methodology, encompassing techniques such as centrifugal atomization^[18], plasma rotating electrode processing^[19], and electrode induction melting gas atomization^[20], necessitates the establishment of a sophisticated equipment infrastructure, which consequently escalates the production costs for titanium.

The processes above utilize sponge titanium or titanium powder as raw materials for preparing Ti-Al alloys, which demands strict quality control of the inputs. Presently, the Kroll process is the predominant method for titanium production. It involves the chlorination and refining of titanium-containing materials, followed by using magnesium as a reducing agent to reduce the $TiCl_4$, ultimately producing metallic titanium. Nevertheless, this process exhibits several deficiencies, including long preparation time, low efficiency, discontinuous production, and the drawbacks of high reaction temperature and equipment corrode^[21-22]. Considering the cost-efficiency of titanium production, it is crucial to use economical raw materials for Ti-Al alloy fabrication.

Given this, there is an increasing research focus on the preparation of Ti-Al alloys utilizing TiO_2 as a raw material. Yan et al^[23] proposed a new method for preparing Ti-6Al-4V powder using a multistage deep reduction technique. They utilized TiO_2 , V_2O_5 , and Al as raw materials, with Mg and Ca as reducing agents. By employing this multistage deep reduction method, they could produce porous Ti-Al-V-O precursor materials with oxygen content ranging from 6.74wt% to 16.4wt%, when the amount of the reducing agent Mg was optimized. After subjecting this precursor to a calcium thermal deep reduction (held at 1173 K for 3.5 h), Ti-6Al-4V powder with an oxygen content of 0.24wt% was obtained. However, the reducing agent used in this process is expensive, and separating the alloy product from by-products is difficult. Aluminum is a more cost-effective reducing agent and can form intermetallic compounds with titanium relative to calcium and magnesium. Employing the aluminothermic reduction process, Maeda et al^[24] successfully synthesized a Ti-Al alloy with a titanium content of 68.9wt% at a temperature of 1973 K, using TiO_2 as the starting material, aluminum as the reductant, CaO as the slag-forming agent, and CaF_2 as a flux. Stoephasius et al^[25] found that the addition of a certain

amount of Ca and CaF_2 to the raw materials during the synthesis of Ti-Al alloy by aluminothermic reduction and electro-slag remelting can reduce the oxygen content in the alloy. Further, Li^[26] investigated the aluminothermic reduction of TiO_2 using different fluxes, including CaO and a combination of CaO- CaF_2 , to produce Ti-Al alloy ingots through slag-metal separation. The findings concluded that calcium oxide can reduce the activation energy for the aluminothermic reduction of TiO_2 . However, the separation of slag and alloy and the quality of the produced alloy were less than ideal.

Based on the above research, this study utilizes MgF_2 as an additive to reform the process of preparing Ti-Al alloy by the aluminothermic reduction of TiO_2 . The influence of MgF_2 addition on the alloy-slag separation, the recovery rate of titanium, the quality of the alloy metal ingots, and the dynamics of aluminothermic reduction have been investigated.

2 Experiment

In this research, the following reactants and auxiliary materials were purchased from Xingrongyuan Technology Co., Ltd (China): titanium dioxide rutile powder (TiO_2 , 99wt% pure, particle size of 80–150 μm), calcium oxide powder (CaO, 99wt% pure, particle size of 80–120 μm), magnesium fluoride powder (MgF_2 , particle size of <50 μm), and aluminum powder (Al, 99.5wt% pure, particle size of <50 μm). Additionally, the calcium oxide powder was calcined at 950 °C for 2 h to remove CO_2 and H_2O from CaO.

Fig.1 shows the schematic of TiAl alloy fabrication process in this research. The experimental reduction commenced with the preparation of the reaction mixture containing 1 mol TiO_2 , 1.21 mol CaO, 2.33 mol Al, and MgF_2 in varying molar quantities. A stoichiometric quantity of 1.21 mol CaO was carefully selected based on empirical evidence to enhance the separation of alloy from slag, while the addition of 2.33 mol Al aimed to facilitate the reduction of TiO_2 and the subsequent synthesis of Ti-Al intermetallics. Furthermore, the study explored the influence of MgF_2 content, ranging from 5wt% to 25wt%, on the synthesis efficiency and resultant properties of Ti-Al alloy.

During the typical experimental procedure, the batch of raw materials was subjected to mechanical mixing using a ball mill within a controlled nitrogen environment. The mill operated at a rotation speed of 200 r/min for 10 min. Following the milling process, the derived powder mixture was subsequently densified utilizing a press, applying a consistent pressure of 20 MPa for a dwell time of 5 min. A preliminary treatment of zinc stearate powder was employed to inhibit adhesion between the mixture and the die during compaction. After the compaction, the formed samples were transferred to a crucible within a silicon-molybdenum resistance furnace. Before the heating, the furnace environment was purged with high-purity argon gas, maintaining a pressure of 0.15 MPa. Then the heating process progressed to 1550 °C at a rate of 10 °C/min and was sustained for 30 min to afford complete reduction and

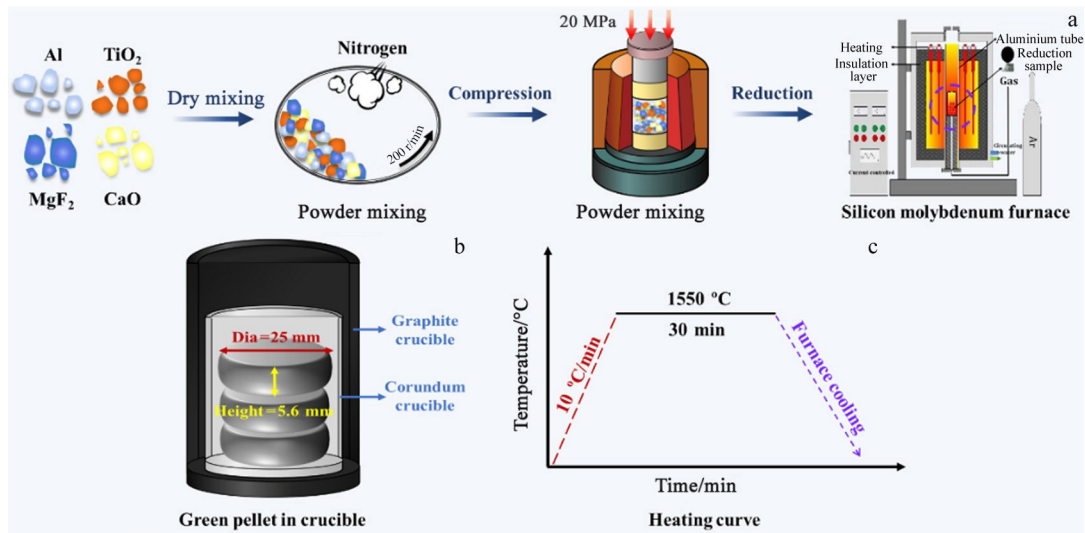


Fig.1 Schematic diagram of Ti-Al alloy fabrication process

effective separation of the alloy from slag. After the reduction hold, the furnace was allowed to naturally cool to room temperature.

The resultant products were identified using X-ray diffraction (XRD) with Cu-K α radiation. The morphology and structure of the final samples were examined using scanning electron microscope (SEM) configured for energy-dispersive X-ray spectroscopy (EDS) analysis. The composition of related elements was quantified using inductively coupled plasma-atomic emission spectrometry (ICP-AES). A thermogravimetric analyzer coupled with differential scanning calorimetry (TG-DSC) was employed to assess the mass loss, heat flux, and reaction onset during the initial reduction process.

3 Results and Discussion

3.1 Effect of MgF₂ on separation process

Fig.2 provides a detailed surface macroscopic morphology of the unseparated samples after aluminothermic reduction under varying conditions: one sample incorporating MgF₂ and a control without the addition. In Fig.2a, it can be observed that the absence of MgF₂ correlates with a pronouncedly

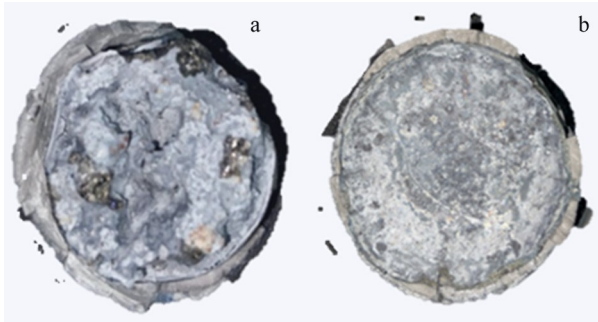


Fig.2 Macroscopic morphologies of slag surface before (a) and after (b) adding MgF₂

rough and porous surface of the slag, beset with multiple metallic inclusions. Such a textural manifestation indicates the ineffectual separation of the resultant alloy from the slag. To rectify this issue, MgF₂ was employed as a slag conditioner to promote superior separation. Fig. 2b depicts the altered morphological characteristic, detailing the surface of slag with MgF₂ addition. The morphology reveals that the enriching presence of MgF₂ results in a notably refined slag texture without discernible metallic inclusions, providing a marked morphological divergence from the sample shown in Fig.2a. This marked transformation underscores the significance of MgF₂ as a flux for enhancing alloy-slag separation. However, the precise mechanistic contributions of MgF₂ to the separation process necessitate further investigation.

Subsequent analysis focused on experimental samples synthesized with MgF₂ additions ranging from 5wt% to 25wt%. Fig.3 presents the macroscopic morphologies of these samples after being comminuted. Observations from Fig. 3 suggest a non-monotonic evolution of the alloy's surface texture with increasing MgF₂ content, transitioning from rough to smooth and reverting to a coarse finish at the highest additive concentrations. In predominant samples, alloy ingots crystallize into consistent elliptical geometries, aggregating at the crucible base enveloped within a slag matrix. Exceptionally, the ingot with MgF₂ addition concentration of 25wt% exhibits a typical morphology with a notably disparate outline. Furthermore, ingots with MgF₂ at the threshold concentrations of 5wt% and 25wt% are covered by a superficial slag veneer, diminishing the intrinsic metallic sheen. Furthermore, an exclusive presence of dispersed metallic particles is noted within the slag matrix of the samples containing 15wt% and 20wt% MgF₂, a feature absent in slags of other compositions.

Parallel to the trends noted in the alloy, slag morphological and structural changes manifest along a similar rough-smooth-rough trajectory in response to escalating MgF₂ content. The initial rise in MgF₂ content precipitates a transition

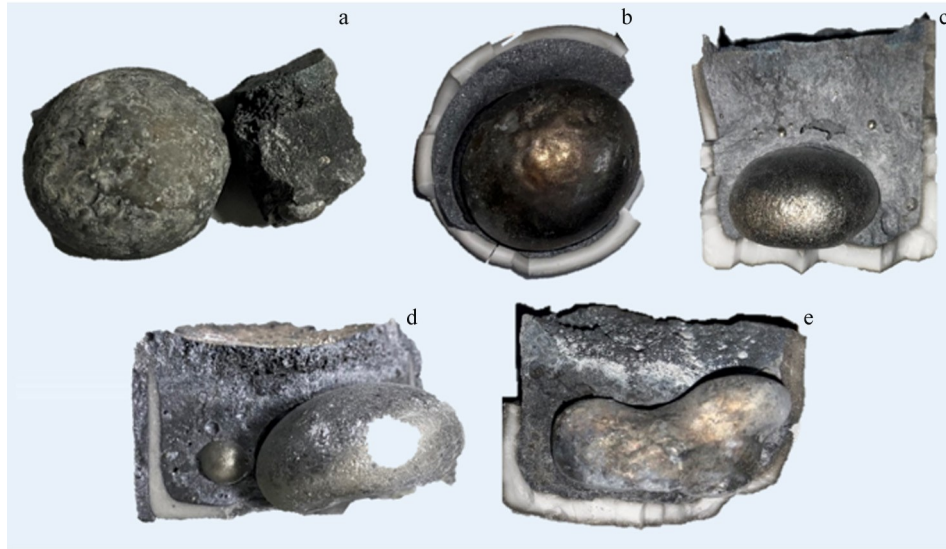


Fig.3 Macroscopic morphologies of experimental samples synthesized with different MgF_2 addition concentrations: (a) 5wt%; (b) 10wt%; (c) 15wt%; (d) 20wt%; (e) 25wt%

towards a more compact and uniform slag texture, which subsequently deteriorates to a rougher and heterogeneous state. Significantly, the slag samples with 5wt%, 20wt%, and 25wt% MgF_2 addition concentrations demonstrates a progressive increase in porosity, and the sample containing 25wt% MgF_2 exhibits notably higher porosity than the others.

The analysis indicates that MgF_2 facilitates the separation of the alloy from the slag. This improvement in separation efficiency is positively correlated with increasing MgF_2 concentrations up to an optimal threshold, beyond which any further addition results in diminished separation performance.

To further elucidate the mechanism behind the impact of MgF_2 on the separation efficacy between slag and alloy, the application of Stokes' Law^[27] was instrumental. This principle was employed to assess the separation rate of metal droplets from the molten slag and can be articulated as follows:

$$V_T = \frac{2gr^2}{9\eta}(\rho_m - \rho_s) \quad (1)$$

where V_T is the alloy droplet settling velocity (m/s); ρ_m is the slag density (kg/m^3); ρ_s is the alloy density (kg/m^3), r is the alloy droplet radius (m); η is the slag kinetic viscosity (Pa·s); g is the acceleration of gravity (m/s^2). This formula suggests that the separation velocity is inversely proportional to the slag's viscosity and directly proportional to the difference in density between the slag and the alloy. Therefore, the effects of MgF_2 on the slag's density and viscosity warrant detailed discussion.

In this study, a binary $\text{CaO-Al}_2\text{O}_3$ slag system is developed through the interaction between CaO and the oxidation product Al_2O_3 , with a focused goal to prevent the formation of a solid Al_2O_3 layer that inhibits further aluminothermic reduction by encasing TiO_2 . This study strategically adjusts the amount of CaO added to ensure a lower melting point for the slag, facilitating continuous reduction. However, challenges emerge, as highlighted by research of Dou et al^[28],

where such a slag composition could lead to increased melting points and viscosity, potentially compromising the quality of the resulting alloy.

Within the circumstance of $\text{CaO-Al}_2\text{O}_3$ -based slag, the consumption of free O^{2-} ions and metal cations leads to the formation of $[\text{AlO}_4]^{5-}$ tetrahedra, which is a reaction driven by the charge compensation effect of Al^{3+} ions^[29]. This process generates networks of Al-related structures, which escalates the degree of polymerization (DOP) within the slag melts, manifesting as significantly increased viscosity and diminished fluidity of the slag.

However, incorporating MgF_2 into slag introduces F^- that substitutes oxygen atoms in $[\text{AlO}_4]^{5-}$ networks, yielding $[\text{AlF}_6]^{3-}$ and $[\text{AlO}_6]^{9-}$ octahedra with a decreased DOP^[30]. The F^- behaves similar to free O^{2-} ions, acting as network modifiers that reduce the viscosity of melt. This can be expressed as the reaction: $3[\text{AlO}_4]^{5-} + 6\text{F}^- = [\text{AlF}_6]^{3-} + 2[\text{AlO}_6]^{9-}$. Consequently, adding 5wt%–25wt% MgF_2 to slag, as computed via FactSage thermodynamic calculation software, demonstrates a substantial reduction in viscosity, as illustrated in Fig. 4a. Significantly, the viscosity diminishes when MgF_2 content exceeds 10wt%, particularly at temperature below 1500 °C. However, the decrease in viscosity plateaus with the further increase in both MgF_2 concentration and temperature.

Meanwhile, the density of the five slag samples was calculated using Eq. (2) as follows:

$$\rho_s = \sum x_i \rho_i \quad (2)$$

where x_i is the mass percentage of each component in the slag; ρ_i is the density of each slag component (kg/m^3). The calculation data of ρ_i come from FactSage. Fig. 4b presents the calculated results, demonstrating a decrease in slag density with increasing MgF_2 content.

The analysis suggests that increased MgF_2 content leads to lower slag viscosity and density, consequently enhancing its fluidity and facilitating the sedimentation of alloy droplets.

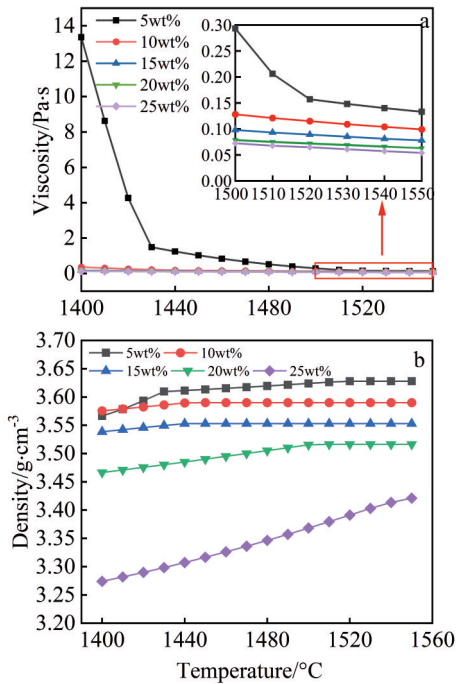


Fig.4 Viscosity (a) and density (b) curves with temperature for slag samples with different MgF₂ content

Building upon this analysis, one would anticipate an enhancement in the separation of alloy from slag concomitant with the increase in MgF₂ content. However, this trend is disrupted when MgF₂ addition reaches 20 wt% and 25 wt%, as evidenced in Fig. 2. Furthermore, recovery efficiency of the alloy, Ti, and Al is derived from the Ti/Al mass ratios in the synthesized alloys, determined by ICP analysis, as depicted in Fig. 5. The recovery rates for Ti generally exceed those for Al, which can be attributed to relatively lower density of Al and higher loss to the slag. Yet, an increase in MgF₂ content is observed to depress recovery rates of Ti and Al generally. Notably, the recovery rate plummets below 50% upon adding 25wt% MgF₂.

MgF₂ also reduces the interfacial tension between the slag and molten Al, promoting the formation of new phase

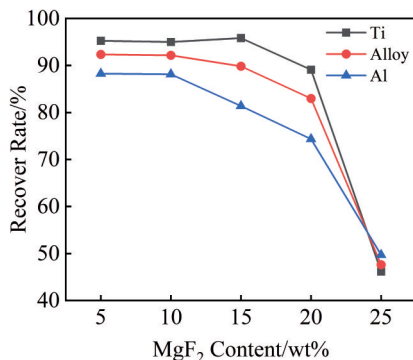


Fig.5 Recovery rate of Ti, Al, and alloy in Ti-Al alloys prepared with different MgF₂ addition concentrations

interfaces. Typically, the viscosity of slag is over an order of magnitude greater than that of liquid metals, leading to a higher degree of dispersion or emulsification of the Al droplets within the slag. Concurrently, with intense chemical reactions at the metal-slag interface, there is a marked decrease in interfacial tension, leading to spontaneous droplet spreading initially, followed by recovery as the reaction rate subsides^[31]. Given these reasons, an overabundance of MgF₂ may result in substantial Al loss and incomplete reduction of TiO₂, culminating in a marked decrease in overall alloy recovery efficiency. The shortfall in reduction potentially results in a slag composition that is low in Al₂O₃ and high in TiO₂. TiO₂ and MgF₂ are recognized for reducing slag surface tension and fostering slag foaming, which hinder efficient alloy separation^[32]. Moreover, decreased surface tension leads to the formation of alloy ingots with irregular shapes.

To summarize, the addition of MgF₂ enhances the efficient partitioning of slag from alloy. Nonetheless, with elevated MgF₂ content, both the viscosity and density of the slag do not achieve the expected parameters, and the decrease in surface tension further impairs the separation efficiency between slag and alloy, resulting in a significant reduction in alloy production yield. Based on the preceding analysis, the sample containing 10wt% MgF₂ exhibits the optimal separation between slag and alloy and a better alloy recovery rate.

3.2 Effect of MgF₂ on synthesized alloy ingots

Furthermore, the effect of MgF₂ on the properties of alloy products deserves exploration. To this end, XRD phase analysis was performed on the Ti-Al alloys synthesized from the five products under consideration, with results shown in Fig. 6. The analysis reveals that the predominant phase in most alloy products is TiAl, followed by Ti₃Al as the secondary phase. As MgF₂ content increases, the peak intensity of the TiAl phase initially rises, peaking at MgF₂ content of 10wt%, suggesting that MgF₂ provides a favorable environment for the formation of the TiAl intermetallic compound. In comparison, the Ti₃Al phase exhibits weaker peak intensities, implying its lower content in the alloy. With increasing MgF₂, the peak corresponding to Ti₃Al gradually intensifies, becoming predominant at the MgF₂ content of 25wt%. This phenomenon can be attributed to excessive MgF₂ causing aluminum depletion, resulting in an increased Ti/Al ratio in the alloy,

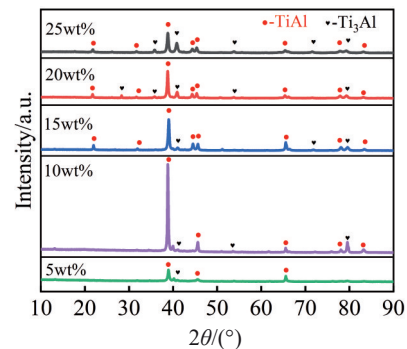


Fig.6 XRD patterns of alloy products with different MgF₂ addition concentrations

thereby promoting the dominant formation of the Ti_3Al phase.

SEM and EDS analyses of the polished samples are detailed in Fig. 7. SEM images reveal three distinct microstructures within the alloy ingots. The primary structure, marked with red region and spot ①, constitutes the alloy matrix. This structure is dense and demonstrates a considerable level of uniformity. EDS analysis for spot ① reveals a molecular ratio of Ti/Al near 1, suggesting the presence of the TiAl intermetallic phase, as corroborated by XRD results. The secondary structure, marked with a yellow region and spot ②, corresponds to the Ti_3Al phase, as evidenced by the Ti/Al molecular ratio from EDS data and XRD analysis. It is observed that Ti_3Al is slightly elevated above the TiAl matrix surface. This elevation difference is attributed to the higher hardness of Ti_3Al , which likely causes it to be less affected during polishing, thus remaining slightly protruding. Lastly, the third structure is marked with the purple region and spot ③, presenting as dark, irregular, and blocky with a dispersed distribution, accompanied by visible pores and cracks. This phase is identified as Al_2O_3 through elemental distribution analysis, indicating incomplete separation from

the alloy matrix. The Al_2O_3 content across the samples also indicates the extent of separation between the alloy and slag.

SEM morphology analysis across five samples reveals that as MgF_2 content increases, the presence of oxide inclusions in the alloy initially decreases and then escalates, with the inclusions enlarging and cracks emerging. Notably, at the MgF_2 content of 10wt%, the alloy exhibits a minimal amount of inclusion and lacks conspicuous cracks. This aligns with the conclusions drawn from the analysis of the separation effectiveness of alloy from slag discussed in the previous section. It can be considered that the quality of the alloy produced at this content of MgF_2 is optimal.

3.3 Kinetic analysis on aluminothermic reduction of TiO_2 with MgF_2 addition

TG-DSC analysis of the sample containing 10wt% MgF_2 was conducted to clarify the mechanism of the aluminothermic reduction process enhanced by MgF_2 . The analysis was performed in an argon environment, spanning temperature from 200 °C to 1400 °C at a heating rate of 10 °C/min. DSC-TG curve, depicted in Fig. 8, revealed four distinct enthalpic signals across this temperature range,

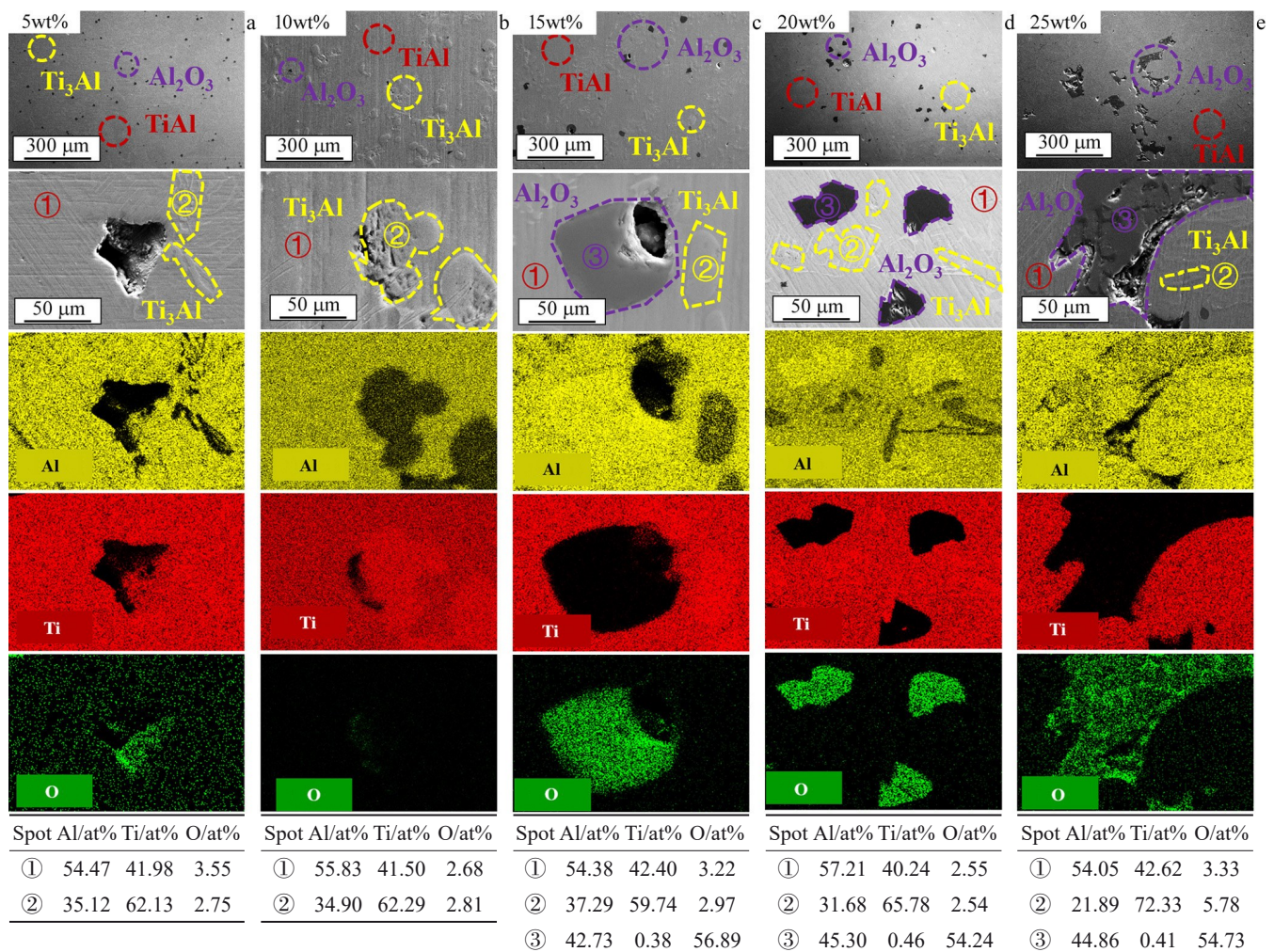
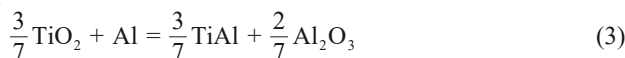


Fig.7 SEM images and EDS results of alloy products with different MgF_2 addition concentrations: (a) 5wt%; (b) 10 wt%; (c) 15wt%; (d) 20wt%; (e) 25wt%

comprising one exothermic and three endothermic signals. The initial endothermic response, identified at 399 °C and marked by significant mass loss, signals the beginning of the melting and subsequent evaporation of MgF₂, which is supported by XRD analysis of volatile compounds. This phenomenon occurs when CaO, upon air exposure, undergoes hydration, absorbing moisture and forming Ca(OH)₂. At approximately 400 °C, Ca(OH)₂ begins decomposition, releasing water vapor and reverting to CaO. The second endothermic signal observed at 653 °C, close to the melting point of aluminum (660 °C), indicates the melting of aluminum. TiO₂ persists in its solid state in this range, enabling a solid-liquid reaction at a comparatively slow rate. The heat generated by the aluminothermic reduction of TiO₂ offsets a fraction of the energy needed for aluminum melting, leading to the noted leftward shift in this endothermic peak. The third endothermic peak, occurring at 1164 °C, corresponds to the MgF₂ melting peak (1225 °C) due to the heat released during the reduction process. The third endothermic peak, observed at 1164 °C, is related to the expected melting peak of MgF₂ at 1225 °C, with its leftward shift caused by heat release during the reduction process. Finally, an exothermic signal was observed at 1301 °C, which is speculated to result from the molten MgF₂ enhancing the heat and mass transfer capabilities of system. This enhancement facilitates the reduction reactions between liquid Al and solid TiO₂. In addition, the wettability between liquid Al and solid TiO₂ is improved with increasing temperature, leading to more uniform diffusion of liquid Al across solid TiO₂ distribution, thereby creating more favorable conditions for reduction kinetics. The two factors significantly enhance the thermal reduction of TiO₂ by Al, resulting in the substantial release of heat.

In summary, the aluminothermic reduction of TiO₂ is a heterogeneous liquid-solid reaction in this study, and the specified formula is as follows:



The kinetics of this process is analyzed using the unreacted core model. The exothermic peaks appearing in DSC curves of the Al-TiO₂ reaction system between 1480 K and 1660 K

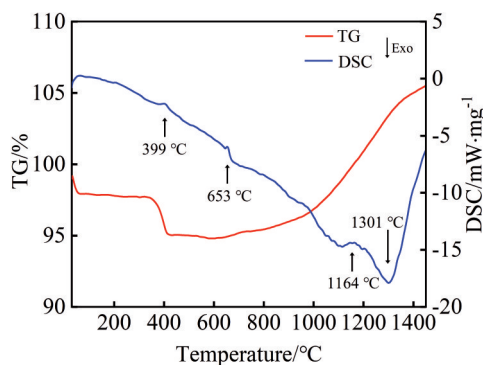


Fig.8 DSC-TG analysis of aluminothermic reduction of TiO₂ with MgF₂ content of 10wt%

are calculated. The typical DSC curve, as shown in Fig. 9, spans from the initial reaction temperature (T_0) to the final reaction temperature (T_c), with the total area under DSC curve designated as S . The area from T_0 to T is marked as S_1 , and from T to T_c as S_2 . According to the Freeman-Carroll differential data processing method, the parameters depicted in Fig.9 adhere to the following equation relationship:

$$\frac{\Delta \lg \Delta T}{\Delta \lg S_2} = -\frac{E}{R} \cdot \frac{\Delta \lg \Delta (1/T)}{\Delta \lg S_2} + n \quad (4)$$

where E is the activation energy, R is the gas constant, and n is the order of kinetics.

By selecting a series of discrete points near the peak and proceeding with linear regression analysis, the $\frac{\Delta \lg \Delta T}{\Delta \lg S_2} - \frac{\Delta \lg \Delta (1/T)}{\Delta \lg S_2}$ relationship curve has been plotted, as shown in Fig.10. From this, the activation energy (E) can be calculated from the slope of the line, and the reaction order (n) can be derived from the intercept of line. After fitting, the linear equation obtained is:

$$y = -21399x + 0.38 \quad (5)$$

This implies the value of $E/2.303R=21399$. The kinetic equation for the reaction between Al and TiO₂ is:

$$\frac{d\alpha}{dT} = \frac{A}{\varphi} (1 - \alpha)^{0.38} \exp\left(-\frac{409.729}{RT}\right) \quad (6)$$

where α represents the rate of change in the chemical reaction, A is the frequency factor, and φ denotes the heating rate. In

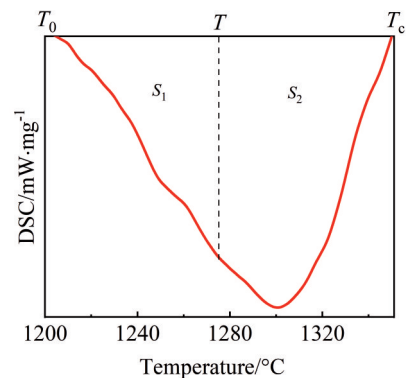


Fig.9 Reaction rate calculated by thermoanalysis

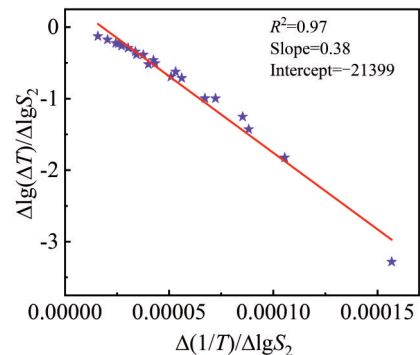


Fig.10 Freeman-Carroll curve of aluminothermic reduction of TiO₂

this study, the activating energy for the Al-TiO₂-CaO-MgF₂ system is 409.729 kJ/mol, and the order of kinetics was $n=0.38$. The activating energy is much smaller than the reaction of Al-TiO₂-CaO^[33], indicating that MgF₂ could decrease the activating energy of aluminothermic reduction.

Overall, the aluminothermic reduction method is considered a viable technique for synthesizing Ti-Al alloys, and further enhancements of this technique could amplify its efficiency as a mechanism for Ti-Al alloy production.

4 Conclusions

1) In the aluminothermic reduction process for producing Ti-Al alloys, the performance of alloy-slag separation is governed by the physical properties of the slag, especially its viscosity and density. The addition of MgF₂ is found to effectively reduce slag viscosity and enhance the density difference between slag and alloy, facilitating separation. However, excess MgF₂ decreases the interfacial tension between slag and metal, leading to increased aluminum loss and incomplete reduction. This deviation from the theoretical slag composition reduces separation efficiency and drastically lowers alloy recovery rates. Within the scope of this study, it has been determined that a MgF₂ content of 10 wt% yields optimal alloy-slag separation and a higher alloy recovery rate.

2) Under the conditions of this experiment, the prepared Ti-Al alloys are primarily in the form of regular-shaped ingots, with the main phase of TiAl and some inclusions of Ti₃Al. However, with the increase in MgF₂ content, the main phase in the Ti-Al alloys shifts from TiAl to Ti₃Al.

3) At MgF₂ content of 10wt% , there is a notable improvement in the aluminothermic reduction of the Al-TiO₂ system. This is evidenced by a decrease in the activation energy of chemical reaction to 409.729 kJ/mol and an enhancement of the kinetics order of 0.38. Such changes suggest that MgF₂ significantly boosts the heat and mass transfer efficiency of system. As a result, it lowers the activation energy required for the aluminothermic reduction of TiO₂ and quickens the overall reaction rate. This underscores the vital function of MgF₂ in enhancing the reaction dynamics of the Al-TiO₂ system.

References

- 1 Froes F H. *Advanced Engineering Materials*[J], 2012, 170(10): 26
- 2 Yamazoe J, Nakagawa M, Matono Y et al. *Dental Materials Journal*[J], 2007, 26(2): 260
- 3 Lai H S, Tang C, Zhong Y et al. *Fatigue & Fracture of Engineering Materials and Structures*[J], 2023, 46(7): 2603
- 4 Qian Y H, Li M S, Lu B et al. *Transactions of Nonferrous Metals Society of China*[J], 2009, 19(3): 525
- 5 Qu X H, Huang B Y, Lu H B et al. *Rare Metal Materials and Engineering*[J], 1991, (4): 3
- 6 Loria E A. *Intermetallics*[J], 2000, 8(9-11): 1339
- 7 Kim Y W, Kim S L. *JOM*[J], 2018, 70(4): 553
- 8 Dimiduk D M, Jms A E. *Materials Science and Engineering A*[J], 1999, 263(2): 281
- 9 Liu F X, He Y H, Liu Y et al. *Rare Metal Materials and Engineering*[J], 2005, 34(2): 169
- 10 Chen Y Y, Ye Y, Zhang Y et al. *Rare Metal Materials and Engineering*[J], 2023, 52(11): 4002
- 11 Liu C T, Wright J L. *Materials Science and Engineering A*[J], 2002, 329: 416
- 12 Bryant J D, Semiatin S L. *Scripta Metallurgica et Materialia*[J], 1991, 25(2): 449
- 13 Imaev R M, Imaev V M, Khismatullin T G et al. *Metallurgy & Metallurgical Engineering*[J], 2006, 48(1-2): 81
- 14 Lee T K, Mosunov E I, Hwang S K et al. *Materials Science and Engineering A*[J], 1997, 240: 540
- 15 Yang B B. *Powder Metallurgy Technology*[J], 1999, 17(4): 286
- 16 Yang J B, Teoh K W, Hwang W S et al. *Materials Science and Technology*[J], 1997, 13(8): 695
- 17 Moll J H, Yolton C F, Mctiernan B J et al. *International Journal of Powder Metallurgy*[J], 1990, 26(2): 149
- 18 Wegmann G, Gerling R, Schimansky F P et al. *Acta Materialia*[J], 2003, 51(3): 741
- 19 Morizono Y, Kumagai R, Nishida M et al. *Materials Transaction*[J], 2003, 44(4): 754
- 20 Wang G, Zheng Z, Chang L T et al. *Acta Metallurgica Sinica*[J], 2011, 47(10): 1263
- 21 Feng Q S, Lv M R, Mao L et al. *Metals*[J], 2023, 13(2): 1
- 22 Fray D J. *International Materials Reviews*[J], 2008, 53(6): 317
- 23 Yan J S, Dou Z H, Zhang T A et al. *Rare Metal Materials and Engineering*[J], 2021, 50(9): 3094
- 24 Maeda M, Yahata T, Mitugi K et al. *Materials Transaction*[J], 1993, 34(7): 599
- 25 Stoephasius J C, Reitz J, Friedrich B et al. *Advanced Engineering Materials*[J], 2007, 9(4): 246
- 26 Li Jun. *Preparation of Ti-based Materials (Ti_nO_{2n-1}, TiAl_{1-n}) by Electric Aluminothermic Reduction of Titanium Raw Materials*[D], Shanghai: Shanghai University, 2018 (in Chinese)
- 27 Zhang Tianan, Dou Zhihe, Xu Shuxiang et al. *Journal of Northeastern University*[J], 2004, 25(2): 142
- 28 Dou Zhihe, Zhang Tingan, Yao Jianming et al. *The Chinese Journal of Process Engineering*[J], 2009, 9(S1): 246 (in Chinese)
- 29 Yan X B, Pan W J, Wang X S et al. *Metallurgical and Materials Transactions B*[J], 2021, 52(4): 2526
- 30 Mills K C, Yuan L, Li Z et al. *High Temperature Materials and Processes*[J], 2012, 31(4-5): 301
- 31 Chung Y S, Cramb A W. *Philosophical Transactions of the Royal Society A*[J], 1998, 356(1739): 981
- 32 Liu Y H, Lv X W, Bai C G et al. *ISIJ International*[J], 2014, 54(10): 2154
- 33 Wang B, Du J J, Liu K R et al. *Journal of Central South University*[J], 2016, 47(11): 3635

MgF₂辅助铝热还原法制备 Ti-Al 合金

田臻贇¹, 陈梁彬¹, 宋晶晶², 康嘉龙¹, 毛红霞¹, 邱贵宝^{1,3}

(1. 重庆大学 材料科学与工程学院, 重庆 400044)

(2. 重庆市计量质量检测研究院, 重庆 401121)

(3. 钒钛冶金及新材料重庆市重点实验室, 重庆 400044)

摘要: 通过添加 CaO 和 MgF₂ 作为助熔剂, 采用铝热还原 TiO₂ 的方法制备了 Ti-Al 合金。研究了 MgF₂ 含量对渣金分离、合金微观结构、成分、相构成、整体合金产率以及 TiO₂ 的铝热还原过程的影响。结果表明, MgF₂ 能够增强合金与渣的分离, 并促进合金基体内 TiAl 相的形成。然而, MgF₂ 的过量添加会减少铝液与渣之间的界面张力, 导致大量铝的损耗。这不利于合金的还原与渣金分离, 增加了合金中氧化物和夹杂物的含量, 严重降低了合金的回收率。同时, 合金的相也从 TiAl 转变为 Ti₃Al。在 MgF₂ 含量为 10wt% 时, 可以实现最佳的合金-渣分离和合金完整性。在这一助熔剂比例下进行的动力学分析确定了 Al-TiO₂-CaO-MgF₂ 体系的活化能为 409.729 kJ/mol, 反应级数为 $n=0.38$ 。

关键词: MgF₂; Ti-Al 合金; 渣金分离; 铝热还原

作者简介: 田臻贇, 男, 1997年生, 博士生, 重庆大学材料与工程学院, 重庆 400044, E-mail: tianzhenyun@cqu.edu.cn